ROYAL SOCIETY
OF CHEMISTRY

Chem Soc Rev

Spin crossover with thermal hysteresis: practicalities and lessons learnt

SCHOLARONE™
Manuscripts

Chemical Society Reviews

TUTORIAL REVIEW

Spin crossover with thermal hysteresis: practicalities and lessons learnt

Sally Brooker

The observation of spin crossover with thermal hysteresis loops of more than a few Kelvin remains relatively uncommon and unpredictable, so is a relatively underdeveloped, but important, area of spin crossover. Lessons learnt regarding the practicalities of the proper study and reporting of thermal hysteresis loops are considered and explained, from a synthetic chemists perspective, herein, after a general introduction to the field of spin crossover.

Introductory remarks and scope

Spin crossover (SCO, Figures 1-4) is currently a hot topic.[1, 2] Particularly active areas include studies aiming to produce compounds with wide hysteresis loops at room temperature,[3, 4] tuning of SCO temperature,[5] multi-step hysteretic SCOs,[6] multifunctional SCO compounds,[7] pressure induced SCO,[8-10] guest dependent SCO (sensors),[11-14] SCO in less common metal ions,[9, 15-17] and probing the movement of the SCO interface through a crystal.[18, 19] In addition, there is rapidly gathering momentum in multidisciplinary studies aimed at producing SCO *materials*, rather than powder samples in vials, as this is an essential, but challenging, step towards the wide array of potential applications of SCO. The materials being explored include nanoparticles (NPs) made up of SCO-active complexes (size usually controlled by use of surfactants)[20, 21] and SCO complexes immobilised on surfaces, either producing relatively soft materials (typically by Langmuir methods[22] or drop casting[23] or sublimation under high vacuum[24-26]) or relatively hard materials (SCO complexes typically *covalently attached* to either a 'flat' surface[27] or a NP[28]; recently a molecular actuator was formed by gluing a single crystal of SCO complex to a support[29]).

This tutorial review firstly provides a general introduction to SCO. There are many excellent recent reviews of SCO so the reader is directed to those for a more detailed introduction to this field, and for a more comprehensive review of the literature.[1, 2, 30] The present review instead focusses in on describing and discussing *thermal hysteresis loops* (Figure 4c) and the many practical points that must be considered when making measurements on complexes exhibiting this behaviour. From discussions at conferences, much of the following appears to be well understood amongst those 'brought up in' large 'permanent' magnetically focussed research groups, but to date key books and reviews in the chemistry literature have not covered these points in detail. This tutorial review attempts to begin to rectify this situation, so that beginners in the field, especially synthetically

focussed researchers like the present author, are made aware of some of these issues and how to deal with them, thus avoiding at least some of the potential pitfalls.

Introduction to basics of spin crossover (SCO)

Octahedral 3d ions with between 4 and 7 electrons can exist in either the high spin (HS, maximum number of unpaired spins) or low spin (LS, minimum number of unpaired spins) configurations, depending on whether the ligand field strength is significantly smaller or larger, respectively, than the pairing energy. Most 3d complexes exist in one or other spin state no matter what the conditions it is studied under. It is only when the field strength is 'just right', not too big and not too small (i.e. in the region of the pairing energy), that SCO can occur. i.e. In this case the application of a perturbation can switch the preferred spin state (Figure 1). A wide range of perturbations can be applied to induce SCO, including a change in temperature, pressure or guest, or laser light irradiation (typically red or green). The last of these is a special case, known as the LIESST effect (light induced excited spin state trapping). It is a slightly different event, involving switching from the LS state to a meta-stable HS state, usually at low temperatures. The relaxation of the meta-stable HS state back to the LS state on warming can be subsequently studied. There are several good reviews of LIESST to which we refer the reader.[31, 32]
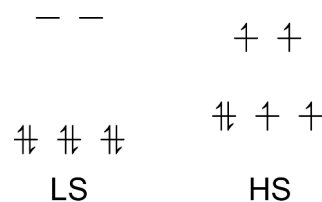

Figure 1. For octahedral iron(II), the diamagnetic LS state and the HS state with 4 unpaired electrons. The LS state is enthalpically favoured whereas the HS state is entropically favoured. SCO occurs when a perturbation causes a switch in spin state HS ↔ LS.

By far the most common way of inducing SCO is by a change in temperature: this is the focus of this tutorial review. The LS state is enthalpically favoured (better bonding, greater CFSE) so stable at lower temperatures, whereas the HS state is entropically favoured (greater electronic and vibrational contributions) so is favoured at higher temperatures ($\Delta G = \Delta H - T\Delta S$).[33] Iron(II), d^6, is by far the most commonly studied metal ion in SCO research (usually with 6N donors), in large part due to the fact that it has the largest possible change in magnetic response,

This journal is © The Royal Society of Chemistry [year]

Chem. Soc. Rev., [year], **[vol]**, 00–00 | **1**

from a diamagnetic LS state to 4 unpaired electrons in the HS state (Figure 1). Hence the spin state is very easily monitored by a magnetometer (NMR spectroscopy can also be used eg. Evans[34] or other method[35]). Many other dramatic changes also occur on
5 SCO at iron(II). Specifically:

(a) The LS state has Fe-N bond lengths (~1.8-2.0 Å) about 10% shorter than in the HS state (~2.0-2.2 Å) as there are no electrons in the antibonding orbitals in the LS state. This can be monitored by X-ray crystallography.[36]

10 (b) Electron density at the nucleus differs for the LS and HS states, so the isomer shift and quadrupole splitting observed in the Mössbauer spectra are very different.[37]

(c) Bond vibrations differ for the two spin states. This is particularly easily seen when NCS (or analogue) is bound to
15 iron(II), as the strong C≡N stretch occurs in an otherwise uncluttered part of the spectrum and is an excellent reporter of spin state (~2100-2140 cm^{-1} LS vs ~2060-2090 cm^{-1} HS). This can be monitored by IR or Raman spectroscopy.[36]

(d) The LS state is typically strongly coloured (eg. purple or dark
20 red), whereas the HS state is typically pale (eg. white or yellow). This can be monitored by UV-vis spectroscopy.[38]

(e) Heat is evolved on SCO from the HS to LS state, and taken up when returning to the HS state.[39, 40] This can be monitored by Differential Scanning Calorimetry (DSC), which also
25 facilitates determination of the ΔH and ΔS for the SCO event.[36, 41, 42]

Due to these changes there are many ways to probe the spin state of the complex.[30] For temperature induced SCO, the spin state can be followed, and the temperature of SCO ($T_{1/2}$, the T at which
30 there is 50:50 HS:LS) determined, by: magnetic, Mössbauer, UV-vis, Raman, IR, NMR, crystallography or DSC measurements, amongst others (eg. tag fluorescence[7]). It is interesting to note that whilst the Fe-N bond lengths may change by around 10%, the unit cell volume change is usually far more modest, as
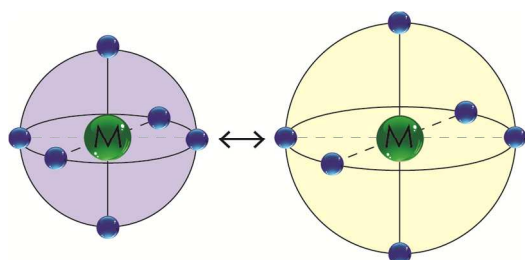35 packing interactions can soak this up and soften the impact.

Figure 2. A schematic illustrating the effect of SCO on an iron(II) coordination sphere: (left) the LS state has bond lengths about 10% shorter than in (right) the HS state. The LS state is usually more intensely
40 coloured (eg. purple or dark red) whereas the HS state is usually paler in colour (eg. colourless, yellow or orange).

SCO at other metal ions also results in significant changes, but usually these are not as dramatic as they are in the case of iron(II). For example, in the case of cobalt(II), the change in
45 number of unpaired electrons is more modest, from 1 in the LS state to 3 in the HS state. However, for cobalt(II) there is an additional point of difference, which is the significant Jahn Teller distortion expected for the LS state. Hence the contraction of bond lengths on switching from the HS to the LS state of
50 cobalt(II) is far less isotropic than it is for iron(II). This is shown

schematically in Figure 3. As cobalt(II) is also well known to undergo valence tautomerism when bound to redox non-innocent ligands,[43] the observation of Jahn-Teller distortion can be very useful to help distinguish SCO[9] from valence tautomerism.
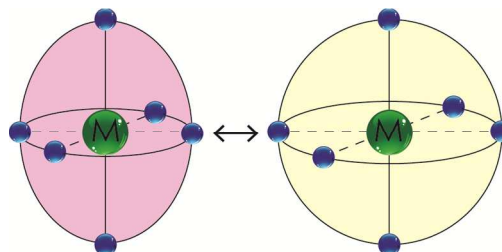

55 Figure 3. A schematic illustrating the effect of SCO on a cobalt(II) coordination sphere: (left) the LS state is expected to show a significant Jahn Teller distortion (shown here as an axial elongation) whereas (right) the HS state is fairly regular. The LS state is usually more intensely
60 coloured (eg. dark port red) whereas the HS state is usually paler in colour (eg. orange).

A variety of SCO profiles are possible (Figure 4). SCO can occur in a complete but gradual manner (Figure 4a) which would be useful for sensing applications, or in an abrupt manner (Figure
65 4b) which would be useful for switching applications. Abrupt means that SCO occurs over just a few degrees (as a result of strong cooperativity); gradual is the opposite, with SCO occurring over many tens of degrees (consistent with a Bolzmann distribution). Complete means 100% conversion from HS to LS
70 and vice versa, which maximises the change. When SCO occurs with thermal hysteresis (Figure 4c and the focus of the remainder of this review) it could be useful for memory applications. Multi-step SCO (Figure 4d) is of interest as this moves one from a molecule acting as a binary switch to a ternary (or greater) switch
75 – so if this occurs with thermal hysteresis (see later) then one would have greater storage density. i.e. instead of a binary memory component one has a three-way (or more) memory component. Gradual and incomplete SCO (Figure 4e) is of less interest. SCO with thermal hysteresis is the focus of the
80 remainder of this review, and a number of different profiles, not just that shown in Figure 4c, are possible, as will be seen later.
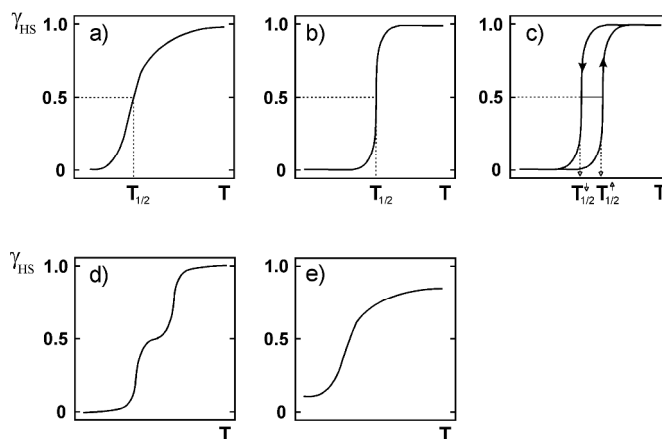

Figure 4. Schematic illustrations of the main types of SCO event, where
85 the y axis is fraction HS (γ, often shown as x) and the x axis is temperature (T): (a) gradual (b) abrupt (c) abrupt with thermal hysteresis (d) two step and (e) incomplete. Reproduced with permission from reference [30]. Copyright 2004 Springer-Verlag.

Introduction to SCO with thermal hysteresis

Thermal hysteresis is a lag in the magnetic response on changing the temperature. It results in a loop in the magnetic susceptibility vs temperature plot for the complex (Figure 4c, and
5 Figure 5 for an example), because the $T_{1/2}$ on the *cooling cycle* ($T_{1/2}\downarrow$) differs from that on the *warming* cycle ($T_{1/2}\uparrow$). Within this loop, the SCO compound is bistable (multi-stability is possible in the case of multi-step SCO compounds[6]), with the spin state depending on its immediate history. i.e. when the sample enters
10 the loop region from the high temperature side it retains the HS state whereas when it enters the loop region from the low temperature side it retains the LS state. These two states can considered as being associated with binary code, on/off, 0/1, so represent a molecular version of a memory component - as after
15 the perturbation (cooling or warming) is applied, it can be removed and the compound returns to ambient temperature (providing this is within the temperature range of the loop) retaining that spin state. To flick the switch from HS to LS requires cooling below $T_{1/2}\downarrow$, whereas from LS to HS requires
20 warming above $T_{1/2}\uparrow$, before allowing it to relax back to ambient temperature (retaining the new spin state). It should be noted that the key difference between a compound that undergoes SCO with thermal hysteresis (memory) and one which 'simply' undergoes SCO, as that the latter is only a switch, as it cannot exist in two
25 different spin states at the same temperature so has no 'memory', so to retain the spin state it must be kept either hot or cold.
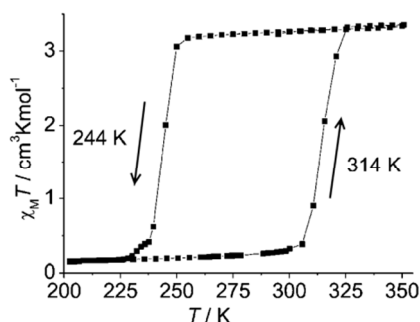

Figure 5. Wide, one-step/simple, thermal hysteresis observed by Weber and co-workers for monometallic [Fe^{II}L(HIm)$_2$]. Importantly the authors
30 specify that this 70 K wide thermal hysteresis loop was measured in 'settle' mode and that it is unchanged on cycling round the loop three times; however no scan rate or relaxation studies are reported. Reproduced, slightly modified, with permission from reference [3]. Copyright 2008 Wiley-VCH.

35 The above description naturally leads to the oft stated aims of those designing and preparing SCO complexes – abrupt, complete and reproducible SCO with a wide hysteresis loop centred around room temperature. Reproducible means that in all cases multiple cooling and warming thermal cycles the magnetic
40 response is unchanged (data points overlay one another in χT vs T plots; Figures 5 & 6). A thermal hysteresis loop centred on room temperature is considered desirable because this is likely to be a useful 'ambient' temperature for futuristic devices based on these nano-memory components (at which it retains its spin
45 state/memory) – and this is one of the key advantages SCO compounds presently have over another class of potential memory components, the Single Molecule Magnets (SMMs), as

the latter currently only show memory at extremely low temperatures (< 14 K[44]).[45, 46] Finally, researchers aspire to
50 generating compounds with wide hysteresis loops, because if the loop is too narrow, a small change in the ambient temperature, such as an atypically hot or cold day, could scramble the memory due to it lying outside of the hysteresis loop temperature range.
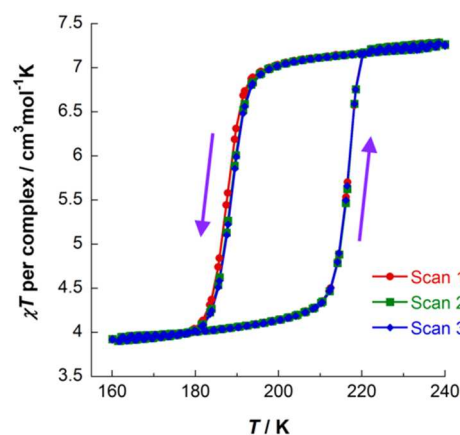

55 Figure 6. χT vs. T data for [Fe^{II}$_2$(PMPh^{tBu}T)$_2$](BF$_4$)$_4$·3.5H$_2$O, obtained on three consecutive cycles around the hysteresis loop, demonstrating its reproducibility. Data acquired in the sweep mode, scanning at 2 K min^{-1}.[41]

What is seldom mentioned is that the *lifetime of the two*
60 *metastable states in the loop region,* and hence *at the temperatures of the loop region*, is another critically important parameter that should also be considered for any memory application. i.e. to be a useful memory component, at the range of intended operating temperatures the $t_{1/2}$ should be at least 10 years.
65 In order to determine this lifetime information it is important that scan rate and relaxation studies be performed, things which are seldom reported at present.

Before considering this point further, examples of different possible thermal hysteresis profiles and selected examples of
70 wide loops are presented. Then some key results from the handful of hysteretic SCO complexes for which significant kinetic analysis of the *thermal* SCO event has been reported,[41, 42, 47-56] are presented as practical illustrations of key points. This develops into a list of practical guidelines for newcomers to the field as to
75 how to best study SCO samples showing thermal hysteresis. For similar reasons, a very simple model of thermal hysteresis,[‡] the Slichter-Drickamer model, is presented. This tutorial review ends with a pictorial summary of some of the different types of effects scan rate can have on thermal hysteresis, and recommendations
80 that magnetic data files, as well as experimental method and analysis/correction details, be routinely supplied as ESI.

State of the art thermal hysteresis loop widths

In contrast to gradual SCO which is a molecular property, abrupt hysteretic SCO occurs in systems which are highly cooperative
85 i.e. the SCO at one centre is communicated effectively to others, either via covalent bridges[6, 57] or strong intermolecular interactions.[54, 58] Thermal hysteresis loops have a variety of shapes, simple (Figure 5&6) and complex/stepped on one or both sides (Figure 7). Some even involve 'reverse-SCO' (Figure 8).
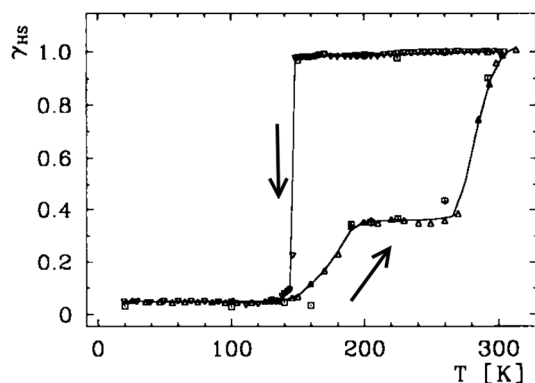
Figure 7. A wide hysteresis loop (ca. 140 K at its widest point; for γ_{HS} = 0.5, $T_{1/2}\downarrow$ = 147 K and $T_{1/2}\uparrow$ = 285 K) structured on the warming side only, reported by Gütlich, Goodwin and co-workers for $[Fe^{II}(3-bpp)_2(CF_3SO_3)_2\cdot H_2O$. HS fraction ($\gamma_{HS}$) derived from the magnetic data (below 140 K, residual γ_{HS} = 0.05). Line just a guide for the eye. Scan mode/rate (settle vs sweep; scan rate) not stated, however relaxation studies are reported. Reproduced, slightly modified, with permission from reference [59]. Copyright 1996 Wiley-VCH.
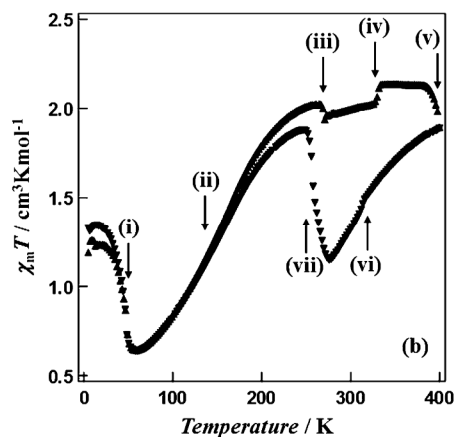

Figure 8. Multiple phase transitions (i to vii at: 49, 160, 269, 330, ca. 400, 314, 258 K) and a wide thermal hysteresis loop (142 K, at the widest point) for a reverse SCO event, reported by Hayami, Ohba and co-workers for $[Co^{II}(C12-terpy)_2](BF_4)_2$. Scan mode/rate (settle vs sweep; scan rate) not stated. No scan rate or relaxation studies reported Reproduced with permission from reference [60]. Copyright 2011 RSC.

Table 1. Selected complexes with wide thermal hysteresis loops, grouped according to nuclearity and within that by loop width. Grey shading indicates unstructured, simple loop structures; pink shading indicates that either tests for reproducibility and/or scan rate studies were reported.

Nuclearity	Complex	ΔT(K)	mode[b]/rate stated?	show its reproducible?	scan rate study?	comments	Ref.
mono	$[Fe^{II}(3-bpp)_2(CF_3SO_3)_2\cdot H_2O$	ca. 140[a]; structured	?/N		No	report relaxation rate study	59
mono	$[Co^{II}(C12-terpy)_2](BF_4)_2$	142[a]; structured	?/N		No	complex shape involves reverse-SCO	60
mono	$[Fe^{II}(L1)_2](BF_4)_2\cdot xH_2O$ (x ≈ 0.5)	130[a]; unstructured	?/N	YES	No	Checked another sample same SCO. Polymorphs different SCO. Faraday balance 80-500 K. DSC at 6Kmin⁻¹.	61
mono	$[Fe^{II}(PM-PEA)_2(NCS)_2]$	37(amb)→100(2.6kbar) unstruct.→struct.	Sweep/YES		YES	1 Kmin⁻¹ at 0.8 T. Say scan rate study done but no details provided. Pressure causes irrev. change and complex loop shape	62
mono	$[Fe^{II}(2-pic)_3]Cl_2\cdot H_2O$	91; unstructured	DSC/YES	YES	No	authors state that loop is 'not genuine but only apparent'	47, 48
mono	$[Fe^{III}(qsal)_2]NCS$	87; structured	Sweep/YES		No	2 Kmin⁻¹ at 0.5 T. Complex shape; loop width given is for second step	63
mono	$[Fe^{II}L(HIm)_2]$	70; unstructured	settle	YES	No		3
mono	$[Co^{II}(dpzca)_2]$	3-14; unstructured	Sweep/YES	YES	YES	Scan rate (10-0.2 Kmin⁻¹) and relaxation rate study; loop closes from both sides as scan rate lowered	9, 56
mono	$[Mn^{III}L1]PF_6$	8; unstructured	Settle/YES	YES	No	current record Mn^{III} hysteresis loop	17
di	$[Fe^{II}_2(L4)_2(meim)_4](meim)_4$	21; unstructured	Settle/N		No	one step [HSHS]-[LSLS]	64
di	$[Fe^{II}_2(PMPh^{tBu}T)_2](BF_4)_4\cdot3.5H_2O$	22-41; unstructured	Sweep/YES	YES	YES	one step [HSHS]-[HSLS]; 0.2-10 Kmin⁻¹ study;. PPMS, DSC & relaxation rate; only cooling branch is scan rate dependent	41
1D-poly	$[Fe^{II}(NH_2trz)_3](NO_3)_{1.7}(BF_4)_{0.3}$	60; unstructured	Optical/N		No	VT SCO monitored at 520 nm	65
1D-poly	$[Fe^{II}(Rtrz)_3](A)_2.xH_2O$ wide range of R and A	3-60 K unstructured loop depending on R & A as well as scan rate	Sweep/YES		YES	Magnetics 0.3 Kmin⁻¹; DSC scan rates 2, 5, 10, 20 Kmin⁻¹	42, 66
2D-poly	$[Fe^{II}(thtrz)_2Pd(CN)_4]\cdot EtOH\cdot H_2O$	2 loops of 19 & 16 K wide; unstructured	Both/YES	YES	YES	Scan rates 1, 1.5, 3, 4 Kmin⁻¹ but no scan rate dependence	6
3D-poly	$\{Fe^{II}(pz)[Pt(CN)_4]\}\cdot 0.5(CS(NH_2)_2)$	56→64→70; unstructured	Sweep/YES		YES	Scan rates 1, 2, 4 Kmin⁻¹ slight scan rate dependence	52

[a] measured at the widest point. [b] settle mode is the gold standard but sweep modes are (faster and) increasingly used. Settle means that at each *T* the device will wait until the *T* has stabilised to within a chosen % before taking the measurement; it is possible to also add a time delay to further ensure the *T* is truly settled. In contrast, for the sweep mode, a temperature sweep rate is set, and the measurements done as the *T* is swept at that rate.

As there are so many different SCO-profiles involved, it is challenging to prepare a table of the best thermal hysteresis loop widths to date. Added to this, the impact of scan rate on loop width is often impossible to assess, due to a lack of detailed information about how the data was collected. Although it is highly likely that experienced magnetochemists collect data in settle mode, often this is not stated, and even when it is, there are still other helpful and informative details that should be provided (what T step was employed and was this constant over the entire range? what was the 'settle' attainment setting – a wait time of x min? or wait until constant χ within y%, or?). However, a selection of leading examples of wide and reproducible *thermal* hysteresis loops is provided (Table 1; please note that consideration of LIESST[31, 32] is not included in this article).

Several different classes of SCO compounds with wide thermal hysteresis can be identified in Table 1, those with the widest *unstructured* loops being either (a) monometallic, two highlights being Bushuev's pyrimidine-based compound (130 K[61]) and Weber's hydrogen-bonded N_4O_2-donor based compound (70 K[3]), or (b) polymeric, including the 1D-polymers of which the triply triazole-bridged 1D-chains[67, 68] are the exemplar (60 K[65]) and 3D-polymers, or frameworks/MOFs, as very nicely illustrated by Real and co-workers (70 K[52]).

The focus in this article is on abrupt thermal hysteresis profiles in which the SCO event occurs in *one step in both directions* as exemplified by the unstructured profile shown in Figures 5 and 6 (not the complex/structured profiles shown in Figures 7 & 8). This cuts out some of the complexes in Table 1, as many have profiles more like those in Figures 7 and 8, in some cases also with far wider loop widths.

The results of scan rate studies have only been reported for a handful of the examples shown in Table 1 (probably because nothing interesting was found; but better practice would be to show these results in the ESI); and only presented in detail for the most recent of these examples.† The importance of scan rate, and of multiple scans, and of correcting for instrumental temperature lag, will be considered in more detail below, as all of these points represent potential traps for newcomers to the field.

Practical advice for newcomers:

Multiple scans and allowing for temperature lag

For all magnetic studies it is very important to keep a wary eye out for batch effects, as variation in crystallinity, solvent content/solvatomorphism,[41] and polymorphism as well as sample age,[69] can all affect the magnetic (in this case SCO) response, often quite dramatically. The results of studies probing these points should be included in the Electronic Supporting Information (ESI) file.

For samples which undergo SCO with thermal hysteresis, an often overlooked point is that the loop should be scanned multiple times as it is not uncommon for the first cycle to result in an irreversible change (for example loss of solvent molecules at the high temperature end of the cycle, as is the case shown in Figure 9), and for the subsequent cycles to therefore be different – and potentially not hysteretic. i.e. after the first cycle the subsequent scans usually overlay one another, but this is not always the case,

so reproducibility should be tested and thereby proven, not assumed. At present the resulting data is seldom presented, and whether or not such a study was performed is often not stated either. This data should be routinely presented in the ESI file (not just archived in house where it is not seen by the community), or presented in the manuscript itself if something interesting is revealed.
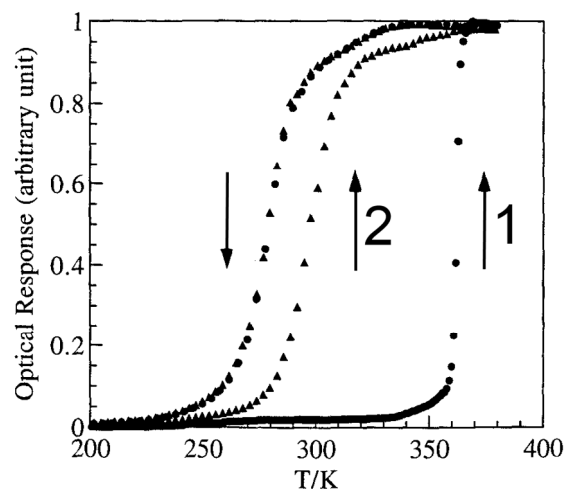
Figure 9. Optical detection of fraction HS vs T for a 1D-chain polymer, which on the first cycle, when hydrated, $[Fe^{II}(NH_2trz)_3](tos)_2 \cdot 2H_2O$, gives a very wide 'apparent' loop (82 K, $T_{1/2}\downarrow$ = 279 K and $T_{1/2}\uparrow$ = 361 K) but on the second cycle, having lost $2H_2O$, the 'real' loop is revealed to be 17 K ($T_{1/2}\uparrow$ is now 296 K). Reproduced, slightly modified, with permission from reference [70]. Copyright 1996 CNRS-Gauthier Villars.

Another key point, very seldom explicitly stated or explained, is that when operating at higher scan rates an additional correction may need to be applied to allow for the temperature lag inherent in the magnetometer/sample system. This is readily done by looking at the cooling vs warming data sets, on both sides of the loop itself, and identifying the $T_{1/2}\uparrow$ and $T_{1/2}\uparrow$ that give the same susceptibility.[56] This should be checked for at each scan rate studied. An example of a correlation obtained in this manner is provided in Figure 10 (NB. the line is only for the eye).
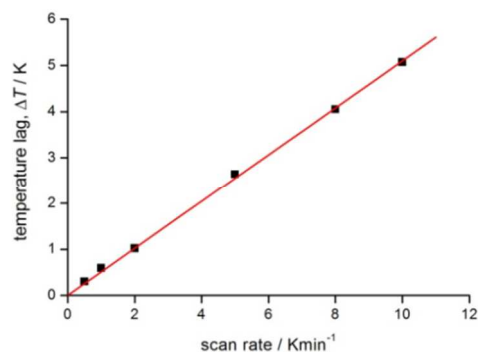
Figure 10. An example of the T(lag) correlation with scan rate for a recent study completed in the authors group. At higher scan rates, the lag is very significant, but even at 2Kmin^{-1} the lag is significant. Reproduced with permission from reference[56]. Copyright 2013 RSC.

This plot illustrates that correcting for this lag can be very important, especially at higher scan rates (as one would expect).

But this is only illustrative, and such a correlation should be obtained for each such study undertaken, as it will depend on the instrument and on the nature and size of the sample. Once the raw data is corrected for this inherent lag, a small 'apparent' loop will

5 likely close as it is not real[36] – so it can be very important to do this. It is also important to show both the raw and corrected data, and to provide all of the details in the experimental section or ESI. Use of a 'settle' mode to collect the data should remove this issue, but most magnetometers are under considerable user

10 pressures these days, so, as 'sweep' mode is far faster and more easily timetabled than settle mode, it is increasingly commonly used (see footnote to Table 1 for definitions of modes).

Scan rate and relaxation rate studies

It is critically important to report the details of the measurement,
15 something which is surprisingly often not done. Specifically, the first point is whether a settle or sweep mode was employed. For the former, the details of the 'settle' setting (eg. set to wait 5 min before taking reading, or to wait until the reading is stable within x%, or?), the size of the temperature steps, and the scan rate used

20 to move between temperatures, should also be provided. For the latter, the 'sweep' mode, the scan rate must be stated.

This information is crucial, as the shape and or position of the loop may well be scan rate dependent, *usually* being *wider at faster scan rates*. This can be seen by consideration of Figure 11,

25 by Roubeau and co-workers, which one of the few examples of such a plot that we have been able to find in the literature. We recently reported another such example, in which the thermal hysteresis loop width of a mononuclear cobalt(II) complex *narrowed from both sides as the scan rate was reduced*, but it did

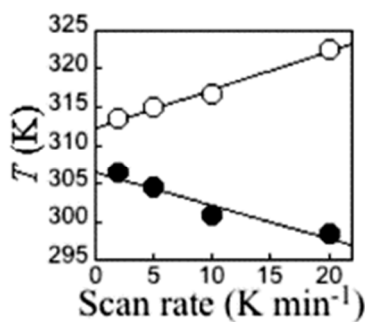30 not close at the rates employed (Figure 12).

Figure 11. A rare example of a scan rate study report on a thermal hysteresis event, for a 1D-chain polymer [Fe^{II}(fatrz)$_3$](NO$_3$)$_2$·H$_2$O by

35 Roubeau and coworkers, showing the expected reduction of the loop width on scanning more slowly. However in this case, and the others reported in this paper, it does not close entirely at the slowest scan speed, despite the expectation that it should close as one approaches zero scan rate (NB. such data should not be linearly extrapolated to zero). .

40 Reproduced with permission from reference [42]. Copyright 2011 ACS.

However, the reverse can also be observed, with a *wider loop being observed at a slower scan rate*. A nice example of this was recently reported by Real and co-workers, for a 'tailed' mononuclear iron(II) complex (Figure 13).[54]

45 In 2000 Hauser and co-workers showed that in the 3D framework complexes [Co^{II}(bpy)$_3$][M^{I}Cr^{III}(ox)$_3$], changing M from Na to Li reduced the size of the cavity occupied by the [Co^{II}(bpy)$_3$]$^{2+}$ cations increasing the 'internal' pressure[71] on them,

stabilising the LS state, and resulting in a change from HS to
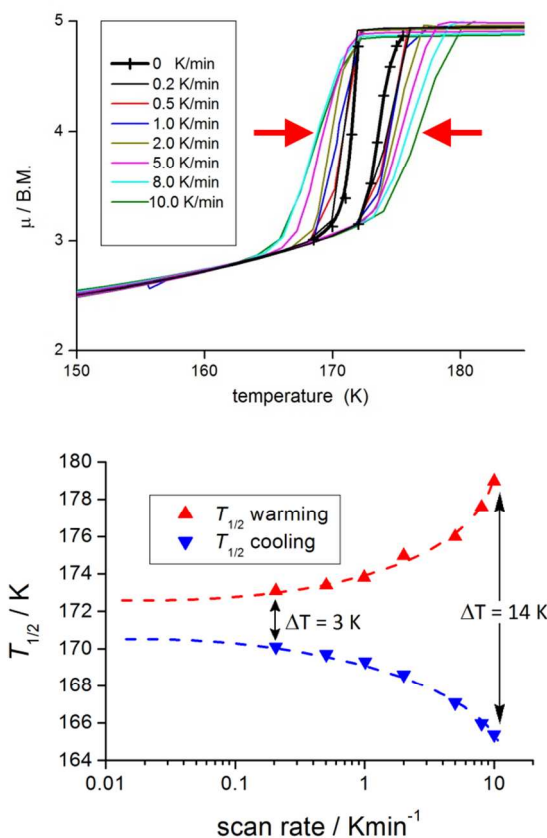50 SCO behaviour.[72] Applying this concept of 'chemical pressure' to

Figure 12. A rare example of a scan rate study report on a thermal hysteresis event, for a mononuclear cobalt(II) complex [Co^{II}(dpzca)$_2$], showing the expected reduction of the loop width on scanning more
55 slowly. However, it does not close entirely at the slowest scan speed, despite the expectation that it should close as one approaches zero scan rate (NB. such data should not be linearly extrapolated to zero). Reproduced, slightly modified, with permission from reference[56]. Copyright 2013 RSC.
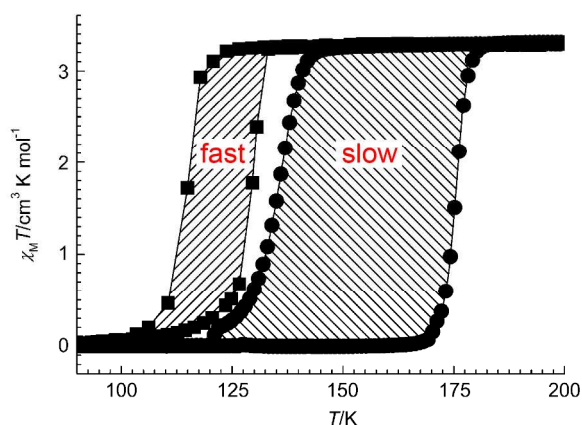

Figure 13. An example of the less common case of a thermal hysteresis loop that widens on scanning more slowly (14 K wide at 4 Kmin^{-1} vs 41 K wide at 0.1 Kmin^{-1}) reported recently by Real and co-workers for monometallic [Fe^{II}(nBu-im)$_3$(tren)](PF$_6$)$_2$. Reproduced with permission
65 from reference [54]. Copyright 2013 Wiley-VCH.

compounds that undergo SCO with thermal hysteresis, it is possible that the cooling branch of the hysteresis loop might be more scan rate dependent than the heating branch, as one generally starts with a HS lattice (at room temperature) and the volume occupied by a LS centre is less than that of a HS centre. Such a scan rate dependence, of only the cooling branch of the thermal hysteresis loop (Figure 14), was reported in a recent study on a dinuclear iron(II) complex, $[Fe^{II}_2(PMPh^{tBu}T)_2](BF_4)_4 \cdot 3.5H_2O$.[41] This caused the hysteresis loop to decrease from 41 K at 10 K min^{-1} to 22 K at 0.2 K min^{-1}, albeit the latter is still a record equalling loop width for a dinuclear complex (Table 1). As for the case shown in Figure 14, clearly the loop does not close even at 0.2 K min^{-1}. Indeed even at that slow rate it remains 22 K wide.
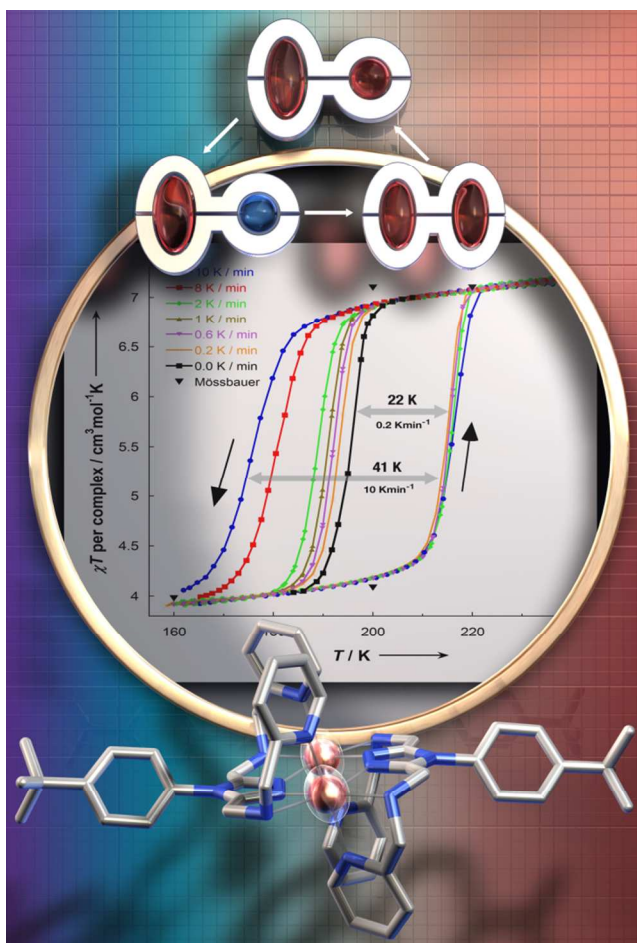

Figure 14. Scan rate dependence of only the cooling branch is seen for $[Fe^{II}_2(PMPh^{tBu}T)_2](BF_4)_4 \cdot 3.5H_2O$, by both χT vs. T (left) and heat flow vs T (right) measurements. Data acquired in the sweep mode, scanning at values in the range 0.2 to 10 K min^{-1}. Reproduced with permission from reference [41]. Copyright 2014 ACS.

Relaxation rate studies were carried out on $[Fe^{II}_2(PMPh^{tBu}T)_2](BF_4)_4 \cdot 3.5H_2O$ in order to probe this further. Specifically, the sample was cooled at 10 K min^{-1} to the desired temperature within the loop, and then the susceptibility was monitored over time whilst temperature was kept constant (Figure 15). This was done at a variety of temperatures, all of which showed a two-step relaxation, consistent with the [HS-HS] to [HS-LS] SCO occurring via an intermediate.[41] Given that far longer relaxation rates, with $t_{1/2}$ of the order of 10 years, are likely required for practical applications, the lifetime of the metastable state(s) should more often be probed and reported. For long lifetimes, the use of magnetometers is probably not feasible as they are in heavy demand, so instead these studies will likely monitor one of the other properties characteristic of the spin state change, such as UV-vis, Raman or IR signals. A recent movie (provided as Supporting Information) showing two identical suspensions of iron(II) nanoparticles in n-octane as the temperature was varied, inducing SCO with a wide thermal hysteresis, nicely illustrated that at the same temperature within the loop they were either colourless (HS) or purple (LS) depending on the history of the sample.[20] In such a case clearly the lifetime of the metastable state could be more readily monitored using changes in colour (i.e. UV-vis spectrum) over time, rather than tying up large amounts of valuable magnetometer time.
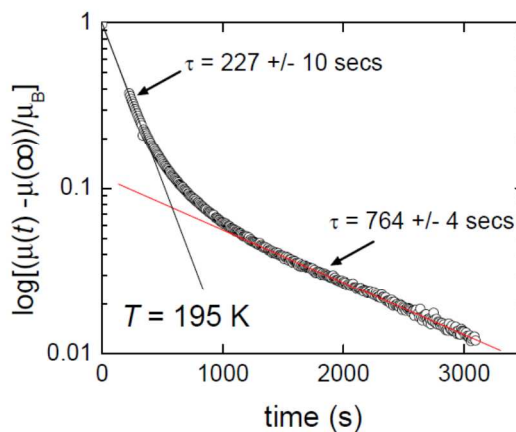

Figure 15. Two step relaxation revealed by time dependence of magnetic moment for $[Fe^{II}_2(PMPh^{tBu}T)_2](BF_4)_4 \cdot 3.5H_2O$ after it was cooled at 10 Kmin^{-1} to 195 K, within the thermal hysteresis loop. Reproduced with permission from reference [41]. Copyright 2014 ACS.

So far, very few plots of $T_{1/2}\uparrow$ and $T_{1/2}\downarrow$ as a function of scan rate have been reported in the literature (Table 1). On discussions with researchers active in this area it seems that such measurements are carried out from time to time but, disappointingly, the results are often not being included in the resulting papers. It would be good to see this change, as even when such studies do not produce 'interesting' results in themselves such a plot should be included in the ESI file – not least as one cannot assume that there is nothing important to see in such a study.

The unprecedentedly wide unstructured thermal hysteresis loop observed by Real and co-workers for the 3D Hofmann type framework $\{Fe^{II}(pz)[Pt(CN)_4]\} \cdot 0.5(CS(NH_2)_2)$ was studied at scan rates of 1, 2, 4 Kmin^{-1}, giving loop widths of 56, 64 and 70 K, respectively, i.e. revealing minimal scan rate dependence for the loop width (Figure 16).[52]
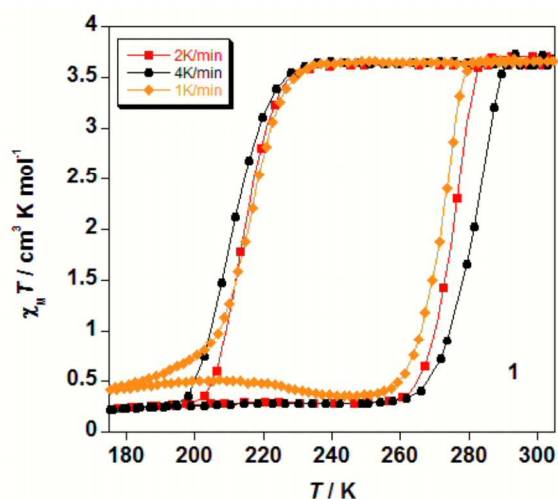
Figure 16. In the 2012 report of 3D Hofmann style framework with a record 60 K wide hysteresis loop, {Fe^{II}(pz)[Pt(CN)$_4$]}·0.5(CS(NH$_2$)$_2$), by Real and co-workers, the supporting information provided a plot showing the impact of scan rate on the SCO response (Table 1). Reproduced with permission from reference [52]. Copyright 2012 RSC.

The flexible 2D Hofmann style framework, [Fe^{II}(thtrz)$_2$Pd(CN)$_4$]·EtOH·H$_2$O, reported this year by Neville, Kepert and co-workers,[6] exhibits a two-step hysteretic SCO[73] (Figure 17): pleasingly the ESI contained figures showing the results for checks of both reproducibility and scan rate dependence (which the authors state in the ESI they carried out in light of reading reference [41]).[6]
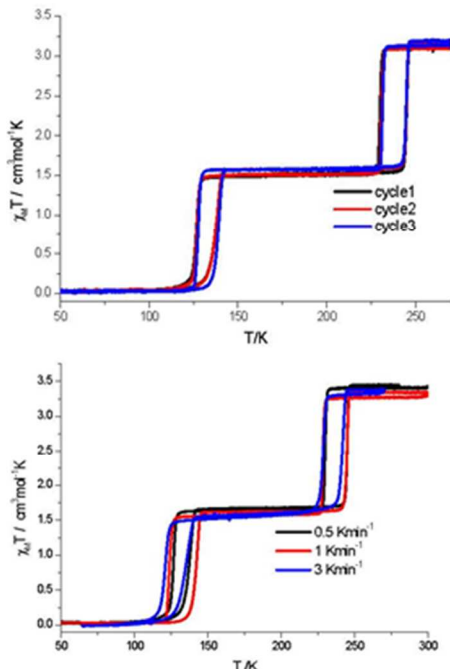

Figure 17. In the case of the 2014 report of flexible 2D Hofmann style framework, [Fe^{II}(thtrz)$_2$Pd(CN)$_4$]·EtOH·H$_2$O, by Neville and co-workers, exhibiting a two-step hysteretic SCO, the supporting information provided plots showing the reproducibility over multiple cycles (top), as well as the minimal impact of scan rate (bottom; NB. carried out on different samples), on the SCO response. Reproduced with permission from reference [6]. Copyright 2014 RSC.

In summary, scan rate and relaxation rate studies are not commonly reported for *thermal* hysteresis events, but the above studies give clear motivation to do, and to report, such studies more often. This is particularly important when interesting SCO profiles are obtained, as relaxation rate and scan rate studies should be used to explore the effect of kinetic factors on the profiles.

Other aspects of thermal hysteresis

Hysteresis is a kinetic effect. A barrier between the spin states arises from cooperative interactions, a crystallographic phase change or other significant structural change, often mediated by strong intermolecular interactions, preventing (rapid) equilibration, even though there may be a large driving force (difference in energy between the spin states). The size of this barrier, and the T$_{½}$↓ & T$_{½}$↑ values, are of key importance to the potential of a given system for use in practical applications. Hence studies that probe the kinetics - scan rate and relaxation studies (see above) – should ideally be carried out and reported for such systems, whether the results prove to be 'interesting' (body of manuscript) or not (ESI).

The basis of abrupt hysteretic SCO is described very nicely in Kahn's landmark book (sections 4.3, 4.4 & 4.7),[74] and can be understood by considering the free energy (G) vs fraction HS (x; hence the fraction LS equals 1-x) plots at a range of temperatures in the loop region. The values of G can be calculated using the Slichter and Drickamer regular solution model (equation 1) which allows for cooperativity between the molecules by use of the mean field interaction parameter (Γ; sometimes represented as γ, which can be confusing as γ is also used at times for the fraction HS; assumed to a first approximation to be independent of T).[75]

$$G = x\Delta H + \Gamma x(1-x) + T\{R[x + (1-x)\ln(1-x)] - x\Delta S \qquad (1)$$

where $G_{LS} = 0$ (by definition).

The details can be obtained from the Kahn book, but the key findings are that when Γ ≤ 2RT$_c$ [where $T_c = ½(T_{½↑} + T_{½↓})$ [ref 42]] the SCO is not hysteretic, but it will be abrupt when Γ = 2RT$_c$, whereas when Γ > 2RT$_c$ the SCO *may* be abrupt and hysteretic. This is because for Γ ≤ 2RT$_c$ situations there is always a unique minimum value of G, in the G vs x plot, whatever the temperature. But for the situation we are interested in, Γ > 2RT$_c$, there is a temperature range ($T_{½↓}$ < T < T$_{½↑}$) in which there are two (unequal except at T$_c$) minima in the curve, close to x = 0 (fully LS) and to x = 1 (fully HS), separated by a maximum (Figure 18), so thermal hysteresis may be observed, with an abrupt SCO (spin transition; ST) occurring at T$_{½↑}$ on the warming branch and at T$_{½↓}$ in the cooling branch.

Outside of the loop temperature range, there should only be one minimum in G. NB. The condition, Γ > 2RT$_c$, is '*necessary but not sufficient*' to ensure hysteresis, as the system must be able to be 'trapped' in the secondary 'metastable' minimum in G.[74] As Halcrow has recently pointed out,[76] there is a tendency to expect that SCO with hysteresis is most likely to be seen when there is also a crystallographic phase change (due to an enhanced barrier/activation energy), however this is not always the case, as

wide hysteresis has been reported for complexes in which there is no phase change.[77] Clearly this is an area in which a deeper understanding remains to be developed; indeed, subsequent to the original submission of this manuscript, a review has appeared in which it is suggested that the primary cause of abrupt SCO is cooperativity - that the symmetry breaking is only an aftermath.[78]
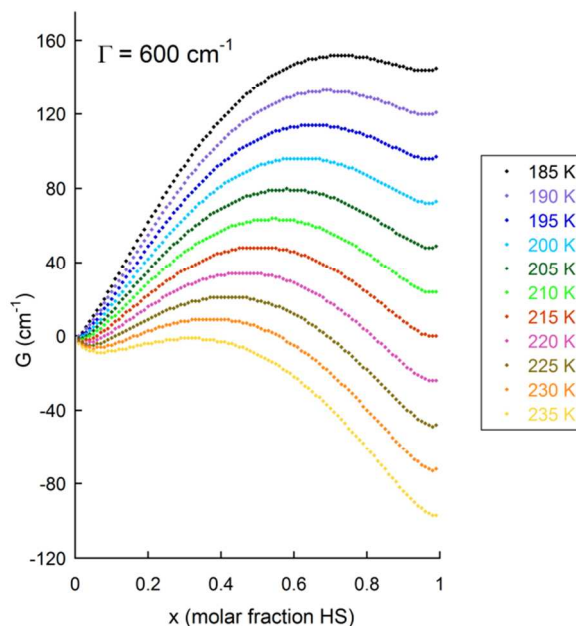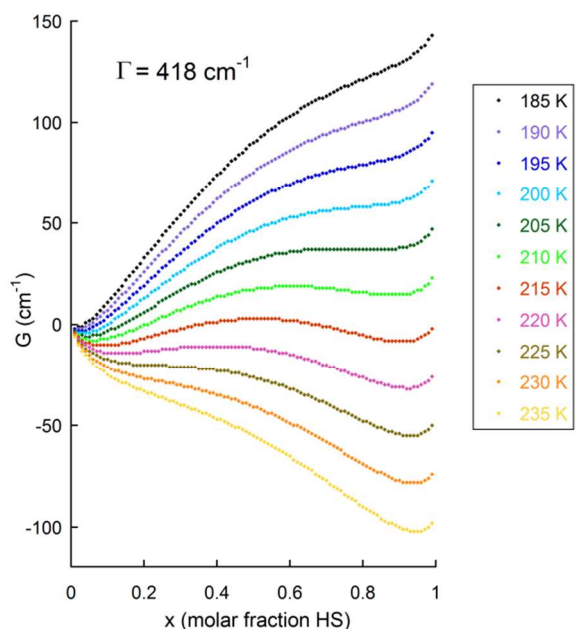

Figure 18. Illustration of the application of the Slichter and Drickamer regular solution model (equation 1[75]) to the data obtained on the abrupt SCO with hysteresis seen for $[Fe^{II}_2(PMPh^{tBu}T)_2](BF_4)_4 \cdot 3.5H_2O$ (see also Figure 14), with (top): observed Γ value of 5 kJmol^{-1} = 418 cm^{-1}, i.e. $\Gamma > 2RT_c$ as $2RT_c \sim 3.3$ kJmol^{-1};[41] and (bottom): for comparison also shown for $\Gamma = 7.2$ kJmol^{-1} = 600 cm^{-1}. The values used to obtain these G values were:[41] $\Delta H = 12.5$ kJmol^{-1} = 1,050 cm^{-1}; $\Delta S = 58$ JK^{-1}mol^{-1} = 4.85 cm^{-1}K^{-1}; $R = 8.314$ JK^{-1}mol^{-1} = 0.69 cm^{-1}K^{-1}; with calculations run at 5 K intervals from 190 to 230 K. NB. for this sample, at the 0.2 Kmin^{-1} scan rate $T_{\frac{1}{2}\downarrow} = 194$ K, $T_{\frac{1}{2}\uparrow} = 216$ K ($\Delta T = 22$ K) whereas at the 10 Kmin^{-1} scan rate $T_{\frac{1}{2}\downarrow} = 175$ K, $T_{\frac{1}{2}\uparrow} = 217$ K ($\Delta T = 42$ K).

In the temperature region within the thermal hysteresis loop, if the activation barrier (maximum in G in each of the G vs x curves) between the two spin states is high enough, and the temperature (at which the curve applies) is low enough, then relaxation to the lower G state can be slow and hence kinetic effects and scan rate dependence can be anticipated.

As can be seen from Figures 18 and 19, the size of the interaction parameter Γ, is one key to whether or not the hysteresis loop will close at slow but still measurable scan rates (one is unlikely to commit the time required on a magnetometer to carry out extremely slow scan rates, eg. << 0.1 Kmin^{-1}). Hypothetically increasing the interaction parameter in these simulations leads to a more significant barrier in G between the LS and HS minima in these curves (and a widening of the loop; see Figure 18 top vs bottom) - but it should be clearly noted that whilst this very simple theory nicely illustrates the overall concept of how hysteresis arises it does not provide a meaningful value for the activation barrier (more advanced theory‡ is required to access the activation barrier height). The other key is the temperature at which the loop occurs, as the effect of the activation barrier will be greater at lower temperatures. If one waited an infinitely long time then all thermal hysteresis loops are expected to close, but experimentally extremely slow scan rates (far slower than standard 'settle' settings) are not usually viable as most magnetometers are in heavy demand.
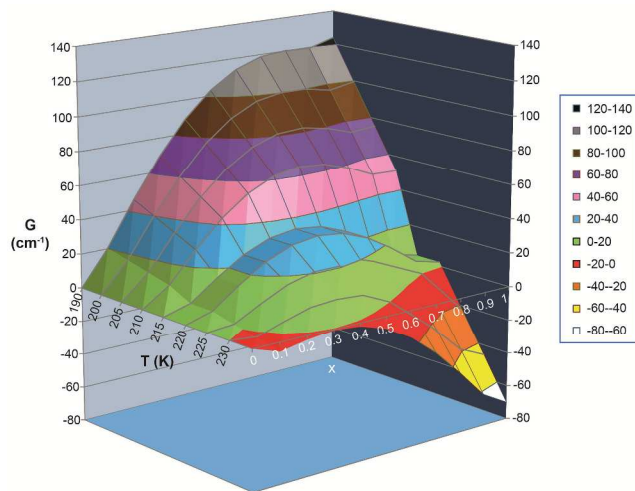

Figure 19. Alternative, 3D plot, of the same data as is shown in Figure 18 top. i.e. with observed Γ value of 5 kJmol^{-1} = 418 cm^{-1}. In this format, it is perhaps easier to see that within the hysteresis loop region there are 2 local minima with a barrier between them, and that which spin state gives the most stable state (i.e. which extreme value of x, 0 or 1, gives the lowest G), and how easy it is to overcome the barrier between them, is temperature dependent. NB. the Slichter and Drickamer model does not give a meaningful barrier height.

For completeness we note that if the activation barrier, maximum in G, is low and the temperature of the loop region is quite high, then relaxation to the lower G state is likely to be fast and little scan rate dependence is expected. Also, that electronic relaxation between spin states should be fast in the absence of cooperativity and/or structural phase changes.[59] It should also be

This journal is © The Royal Society of Chemistry [year]

Chem. Soc. Rev., [year], **[vol]**, 00–00 | 9

noted that whilst another well established model, the Sorai Domain model,[40, 79, 80] cannot model the thermal hysteresis loop itself, it can model the abruptness of SCO in the heating and in the cooling mode, which should result in significantly different domain sizes (hysteresis: n↑ ≠ n↓).[74] Finally, if the reader is interested in the modelling of spin crossover systems, and in obtaining meaningful values for the activation barrier, they are advised to read the many recent papers and reviews covering the considerable progress in this area over recent years.‡

Summary

A variety of scan rate effects on SCO thermal hysteresis events can be observed, and some of these are summarised pictorially in Figure 20.
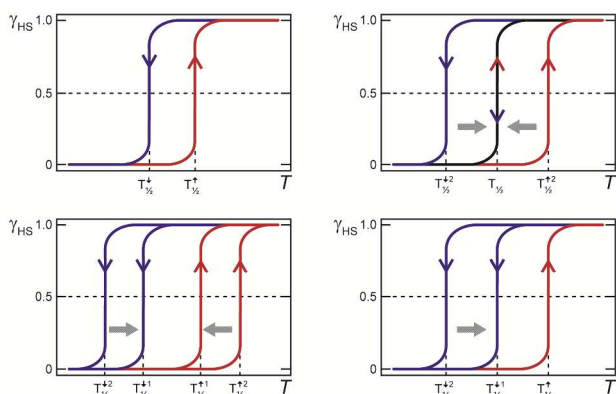
Figure 20. Some of the possible effects of scan rate on a thermal hysteresis loop. Top left: no/almost no effect (long metastable state lifetime); for example see refs [6, 52]. Top right: loop closes at slower sweep rates (short metastable state lifetime). Bottom left: Both heating and cooling modes sweep rate dependent but loop remains open (long metastable state lifetime); for examples see refs [42, 56]. Bottom right: Only the cooling mode is sweep rate dependent so the loop remains open at slow scan speeds (long metastable state lifetimes); for example see ref [41].

It is recommended that samples showing SCO with thermal hysteresis be examined as follows, and the results reported in the ESI, or in the manuscript itself if interesting:

1. Test reproducibility of the SCO response as a function of batch/solvent content/polymorph/crystallinity/age[69] of sample.
2. Test reproducibility of SCO response over multiple cycles.
3. Test for effect, if any, of scan rate on SCO response (important as the loop should ideally remain wide even at very slow scan rate).
4. Carry out relaxation rate studies at temperatures within the loop, as these allow an estimation of the lifetime of the metastable state (important for any practical applications).

Finally, as a consequence of the above recommendations, it is recommended that we (authors and journal editors) learn from the crystallography community, who with great foresight agreed to a common file format (*.cif), established a database (CSD),[81, 82] established the standard practice of providing the data collection and refinement details and cif files as ESI, and thereby ensured that the structural data analysis was refereed and the data readily and widely available. For papers reporting thermal hysteresis it would be good to see:

1. all magnetic datasets (pre- and post-corrections; with correction details noted) provided as ESI files (just as cif files are provided for structures).
2. details of the data collection strategies employed clearly stated (settle vs sweep, T steps, settle requirement, sweep rate, etc).
3. details of all corrections applied to the data mentioned in the text (eg. actual value of the diamagnetic correction applied – and a note as to whether it was calculated from Pascal's constants or from -0.5×10^{-6} x molecular weight; details of T_{lag} determination if this correction is applied).

i.e. It would be good to see the full reporting of experimental magnetic data, with collection details and the actual data files (pre and post corrections) provided as supporting information, become standard practise.

Conclusion

As stated above, to date a key focus of researchers aiming at memory applications of SCO compounds has been to prepare complexes which exhibit thermal hysteresis at room temperature. The scan rate dependence studies and simulations presented above show that another factor should also be considered: the need for the state of the switch to have a reasonable lifetime, preferably >10 years, at the 'ambient' or working temperature of the device, most likely approximately at the middle of the thermal hysteresis loop. This is a more demanding prospect, especially for applications at room temperature. However, for longer lifetimes the next generations of such complexes should feature greater cooperativity between SCO centres (interaction term/domain size). Ideally, future screening for such complexes will include routine reporting of scan rate studies of, and relaxation rate studies within, the thermal hysteresis loop, along with full experimental details and the provision of the data files as ESI.
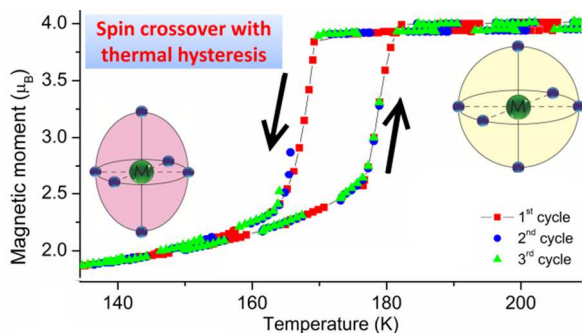
Notes and references

Department of Chemistry and MacDiarmid Institute for Advanced Materials and Nanotechnology, University of Otago, PO Box 56, Dunedin, New Zealand. Fax: +64 3 479 7906; Tel: +64 3 479 7919; E-mail: sbrooker@chemistry.otago.ac.nz

† Perhaps in some cases this was reported in light of hearing the present author's lectures, suggesting this, at the International Conference on Advanced Complex Inorganic Nanomaterials (ACIN), Namur, Belgium, 15-19 July (2013) or more recently at the International Conference on Coordination Chemistry (ICCC-41), Singapore, 21-25 July (2014), or on reading reference [41].

‡ In recent years considerable progress has been made with regard to modelling SCO. See for example references [77, 83-91].

1. P. Gütlich, A. B. Gaspar and Y. Garcia, *Beilstein J. Org. Chem.*, 2013, 9, 342–391.
2. M. A. Halcrow, *Spin-Crossover Materials: Properties and Applications*, John Wiley & Sons, Ltd, 1st Ed. edn., 2013.
3. B. Weber, W. Bauer and J. Obel, *Angew. Chem. Int. Ed.*, 2008, 47, 10098-10101.
4. I. Boldog, A. B. Gaspar, V. Martínez, P. Pardo-Ibañez, V. Ksenofontov, A. Bhattacharjee, P. Gütlich and J. A. Real, *Angew. Chem. Int. Ed.*, 2008, 47, 6433-6437.
5. K. Nakano, N. Suemura, K. Yoneda, S. Kawata and S. Kaizaki, *Dalton Trans.*, 2005, 740-743.
6. Y. M. Klein, N. F. Sciortino, F. Ragon, C. E. Housecroft, C. J. Kepert and S. M. Neville, *Chem. Commun.*, 2014, 50, 3838-3840.
7. Y. Garcia, F. Robert, A. D. Naik, G. Zhou, B. Tinant, K. Robeyns, S. Michotte and L. Piraux, *J. Am. Chem. Soc.*, 2011, 133, 15850–15853.
8. A. Bhattacharjee, M. Roy, V. Ksenofontov, J. A. Kitchen, S. Brooker and P. Gütlich, *Eur. J. Inorg. Chem.*, 2013, 843–849.
9. M. G. Cowan, J. Olguín, S. Narayanaswamy, J. L. Tallon and S. Brooker, *J. Am. Chem. Soc.*, 2012, 134, 2892–2894 and front cover feature.
10. J. Linares, E. Codjovi and Y. Garcia, *Sensors*, 2012, 12, 4479-4492.
11. G. J. Halder, C. J. Kepert, B. Moubaraki, K. S. Murray and C. S. Cashion, *Science*, 2002, 298, 1762-1765.
12. A. Ferguson, M. A. Squire, D. Siretanu, D. Mitcov, C. Mathonière, R. Clérac and P. E. Kruger, *Chem. Commun.*, 2013, 49, 1597-1599.
13. R. A. Bilbeisi, S. Zarra, H. L. C. Feltham, G. N. L. Jameson, J. K. Clegg, S. Brooker and J. R. Nitschke, *Chem. Eur. J.*, 2013, 19, 8058–8062.
14. X. Bao, H. J. Shepherd, L. Salmon, G. Molnár, M.-L. Tong and A. Bousseksou, *Angew. Chem. Int. Ed.*, 2013, 125, 1236–1240.
15. G. G. Morgan, K. D. Murnaghan, H. Müller-Bunz, V. McKee and C. J. Harding, *Angew. Chem. Int. Ed.*, 2006, 45, 7192-7195.
16. S. Hayami, Y. Komatsu, T. Shimizu, H. Kamihata and Y. H. Lee, *Coord. Chem. Rev.*, 2011, 255, 1981-1990.
17. P. N. Martinho, B. Gildea, M. M. Harris, T. Lemma, A. D. Naik, H. Muller-Bunz, T. E. Keyes, Y. Garcia and G. G. Morgan, *Angew. Chem. Int. Ed.*, 2012, 51, 12597–12601.
18. A. Slimani, F. Varret, K. Boukheddaden, D. Garrot, H. Oubouchou and S. Kaizaki, *PRL*, 2013, 110, 087208.
19. M. Sy, F. Varret, K. Boukheddaden, G. Bouchez, J. Marrot, S. Kawata and S. Kaizaki, *Angew. Chem. Int. Ed.*, 2014, 53, 7539–7542.
20. J. R. Galan-Mascaros, E. Coronado, A. Forment-Aliaga, M. Monrabal-Capilla, E. Pinilla-Cienfuegos and M. Ceolin, *Inorg. Chem.*, 2010, 49, 5706-5714.
21. H. J. Shepherd, G. Molnár, W. Nicolazzi, L. Salmon and A. Bousseksou, *Eur. J. Inorg. Chem.*, 2013, 653–661.
22. H. Soyer, E. Dupart, C. J. Gómez-García, C. Mingotaud and P. Delhaès, *Adv. Mater.*, 1999, 11, 382-384.
23. A. Grohmann, M. Haryono, K. Student, P. Müller and M. Stocker, *Eur. J. Inorg. Chem.*, 2013, 662–669.
24. S. Shi, G. Schmerber, J. Arabski, J.-B. Beaufrand, D. J. Kim, S. Boukari, M. Bowen, N. T. Kemp, N. Viart, G. Rogez, E. Beaurepaire, H. Aubriet, J. Petersen, C. Becker and D. Ruch, *Appl. Phys. Lett.*, 2009, 95, 043303.
25. L. Rigamonti, M. Piccioli, L. Malavolti, L. Poggini, M. Mannini, F. Totti, B. Cortigiani, A. Magnani, R. Sessoli and A. Cornia, *Inorg. Chem.*, 2013, 52, 5897−5905.
26. B. Warner, J. C. Oberg, T. G. Gill, F. E. Hallak, C. F. Hirjibehedin, M. Serri, S. Heutz, M.-A. Arrio, P. Sainctavit, M. Mannini, G. Poneti, R. Sessoli and a. P. Rosa, *J. Phys. Chem. Lett.*, 2013, 4, 1546−1552.
27. S. Cobo, G. Molnár, J. A. Real and A. Bousseksou, *Angew. Chem. Int. Ed.*, 2006, 45, 5786-5789.
28. M. Perfetti, F. Pineider, L. Poggini, E. Otero, M. Mannini, L. Sorace, C. Sangregorio, A. Cornia and R. Sessoli, *Small*, 2014, 10, 323–329.
29. H. J. Shepherd, I. A. Gural'skiy, C. M. Quintero, S. Tricard, L. Salmon, G. Molnár and A. Bousseksou, *Nature Commun.*, 2013, 4, 2607.
30. P. Gütlich and H. A. Goodwin, *Top. Curr. Chem.*, 2004, 233, 1-47.
31. S. Decurtins, P. Gütlich, C. P. Kohler, H. Spiering and A. Hauser, *Chem. Phys. Lett.*, 1984, 105, 1-4.
32. F. Varret, K. Boukheddaden, G. Chastanet, N. Paradis and J.-F. Létard, *Eur. J. Inorg. Chem.*, 2013, 763–769.
33. O. Kahn, *Chem. Br.*, 1999, 2, 24-27.
34. D. F. Evans, *J. Chem. Soc.*, 1959, 2003-2005.
35. B. Weber and F. A. Walker, *Inorg. Chem.*, 2007, 46, 6794-6803.
36. H. L. C. Feltham, C. Johnson, A. B. S. Elliot, K. C. Gordon, M. Albrecht and S. Brooker, *Inorg. Chem.*, 2015, DOI: 10.1021/ic503040f.
37. P. Gütlich, *Z. Anorg. Allg. Chem.*, 2012, 638, 15-43.
38. C. Gandolfi, C. Moitzi, P. Schurtenberger, G. G. Morgan and M. Albrecht, *J. Am. Chem. Soc.*, 2008, 130, 14434-14435.
39. M. Sorai, Y. Nakazawa, M. Nakano and Y. Miyazaki, *Chem. Rev.*, 2013, 113 PR41-PR122.
40. M. Sorai, *Top. Curr. Chem.*, 2004, 235, 153-170.
41. R. Kulmaczewski, J. Olguín, J. A. Kitchen, H. L. C. Feltham, G. N. L. Jameson, J. L. Tallon and S. Brooker, *J. Am. Chem. Soc.*, 2014, 136, 878–881.
42. O. Roubeau, M. Castro, R. Burriel, J. G. Haasnoot and J. Reedijk, *J. Phys. Chem. B*, 2011, 115, 3003-3012.
43. T. Tezgerevska, K. G. Alley and C. Boskovic, *Coord. Chem. Rev.*, 2014, 268, 23-40.
44. J. D. Rinehart, M. Fang, W. J. Evans and J. R. Long, *J. Am. Chem. Soc.*, 2011, 133, 14236-14239.
45. D. N. Woodruff, R. E. P. Winpenny and R. A. Layfield, *Chem. Rev.*, 2013, 113, 5110-5148.
46. H. L. C. Feltham and S. Brooker, *Coord. Chem. Rev.*, 2014, 276, 1–33.
47. M. Sorai, J. Ensling, K. M. Hasselbach and P. Gütlich, *Chem. Phys.*, 1977, 20, 197-208.
48. T. Nakamoto, A. Bhattacharjee and M. Sorai, *Bull. Chem. Soc. Japan*, 2004, 77, 921-932.
49. J. A. Rodríguez-Velamazán, M. Castro, E. Palacios, R. Burriel, T. Kitazawa and T. Kawasaki, *J. Phys. Chem. B*, 2007, 111, 1256-1261.
50. C. M. Grunert, H. A. Goodwin, C. Carbonera, J.-F. Letard, J. Kusz and P. Gütlich, *J. Phys. Chem. B*, 2007, 111, 6738-6747.
51. M. Seredyuk, A. B. Gaspar, V. Ksenofontov, Y. Galyametdinov, J. Kusz and P. Gütlich, *Adv. Funct. Mater.*, 2008, 18, 2089-2101.
52. F. J. Muñoz-Lara, A. B. Gaspar, D. Aravena, E. Ruiz, M. C. Muñoz, M. Ohba, R. Ohtani, S. Kitagawa and J. A. Real, *Chem. Commun.*, 2012, 48, 4686-4688.
53. J.-F. Létard, S. Asthana, H. J. Shepherd, P. Guionneau, A. E. Goeta, N. Suemura, R. Ishikawa and S. Kaizaki, *Chem. Eur. J.*, 2012, 18, 5924–5934.
54. M. Seredyuk, M. C. Muñoz, M. Castro, T. Romero-Morcillo, A. B. Gaspar and J. A. Real, *Chem. Eur. J.*, 2013, 19, 6591–6596.
55. G. A. Craig, J. S. n. Costa, S. J. Teat, O. Roubeau, D. S. Yufit, J. A. K. Howard and G. Aromí, *Inorg. Chem.*, 2013, 52, 7203−7209.
56. R. G. Miller, S. Narayanaswamy, J. L. Tallon and S. Brooker, *New J. Chem.*, 2014, 38, 1932-1941.
57. J. Krober, E. Codjovi, O. Kahn, F. Groliere and C. Jay, *J. Am. Chem. Soc.*, 1993, 115, 9810-9811.
58. B. Weber, W. Bauer, T. Pfaffeneder, M. M. Dîrtu, A. D. Naik, A. Rotaru and Y. Garcia, *Eur. J. Inorg. Chem.*, 2011, 3193-3206.
59. T. Buchen, P. Gütlich, K. H. Sugiyarto and H. A. Goodwin, *Chem. Eur. J.*, 1996, 9, 1134-1138.
60. S. Hayami, K. Kato, Y. Komatsu, A. Fuyuhiro and M. Ohba, *Dalton Trans.*, 2011, 40, 2167-2169.
61. M. B. Bushuev, V. A. Daletsky, D. P. Pishchur, Y. V. Gatilov, I. V. Korolkov, E. B. Nikolaenkova and V. P. Krivopalov, *Dalton Trans.*, 2014, 43, 3906-.
62. V. Ksenofontov, G. Levchenko, H. Spiering, P. Gütlich, J. F. Létard, Y. Bouhedja and O. Kahn, *Chem. Phys. Lett.*, 1998, 294, 545-553.

63. S. Hayami, K. Hiki, T. Kawahara, Y. Maeda, D. Urakami, K. Inoue, M. Ohama, S. Kawata and O. Sato, *Chem. Eur. J.*, 2009, 15, 3497-3508.

64. B. Weber, E. S. Kaps, J. Obel, K. Achterhold and F. G. Parak, *Inorg. Chem.*, 2008, 47, 10779-10787.

65. O. Kahn and C. J. Martinez, *Science*, 1998, 279, 44-48.

66. O. Kahn, Y. Garcia, J. F. Létard and C. Mathonière, *Supramolecular Engineering of Synthetic Metallic Materials*, 1999, 127-144.

67. L. G. Lavrenova and O. G. Shakirova, *Eur. J. Inorg. Chem.*, 2013, 670–682.

68. L. G. Lavrenova, V. N. Ikorskii, V. A. Varnek, I. M. Oglezneva and S. V. Larionov, *Koord. Khim.*, 1986, 12, 207.

69. G. A. Craig, J. S. Costa, O. Roubeau, S. J. Teat and G. Aromí, *Eur. J. Inorg. Chem.*, 2013, 745–752.

70. E. Codjovi, L. Sommier, O. Kahn and C. Jay, *New J. Chem.*, 1996, 20, 503-505.

71. A. Hauser, *Chem. Phys. Lett.*, 1992, 192, 65–70.

72. R. Sieber, S. Decurtins, H. Stoeckli-Evans, C. Wilson, D. Yufit, J. A. K. Howard, S. C. Capelli and A. Hauser, *Chem. Eur. J.*, 2000, 6, 361-368.

73. J.-B. Lin, W. Xue, B.-Y. Wang, J. Tao, W.-X. Zhang, J.-P. Zhang and X.-M. Chen, *Inorg. Chem.*, 2012, 51, 9423−9430.

74. O. Kahn, *Molecular Magnetism*, VCH Publishers Inc., New York, 1993.

75. C. P. Slichter and H. G. Drickamer, *J. Chem. Phys.*, 1972, 56, 2142-2160.

76. M. A. Halcrow, in *Spin-Crossover Materials: Properties and Applications*, ed. M. A. Halcrow, John Wiley & Sons, Ltd, 2013, pp. 147-169.

77. M. M. Dîrtu, C. Neuhausen, A. D. N. A. Rotaru, L. Spinu and Y. Garcia, *Inorg. Chem.*, 2010, 49, 5723–5736.

78. M. Shatruk, H. Phan, B. A. Chrisostomo and A. Suleimenova, *Coord. Chem. Rev.*, 2015, DOI: 10.1016/j.ccr.2014.1009.1018.

79. M. Sorai and S. Seki, *J. Phys. Chem. Solids*, 1974, 35, 555-570.

80. T. Nakamoto, Z.-C. Tan and M. Sorai, *Inorg. Chem.*, 2001, 40, 3805-3809.

81. F. H. Allen, S. A. Bellard, M. D. Brice, B. A. Cartwright, A. Doubleday, H. Higgs, T. Hummelink, B. G. Hummelink-Peters, O. Kennard, W. D. S. Motherwell, J. R. Rodgers and D. G. Watson, *Acta Crystallogr. Sect. B*, 1979, 35, 2331-2339.

82. F. H. Allen, *Acta Crystallogr. Sect. B*, 2002, 58, 380-388.

83. C. Enachescu, R. Tanasa, A. Stancu, E. Codjovi, J. Linares and F. Varret, *Phys. B*, 2004, 343, 15-19.

84. S. Ye and F. Neese, *Inorg. Chem.*, 2010, 49, 772-774

85. A. Bousseksou, G. Molnár, L. Salmon and W. Nicolazzi, *Chem. Soc. Rev.*, 2011, 40, 3313-3335.

86. A. Vargas, I. Krivokapic, A. Hauser and L. M. L. Daku, *Phys. Chem. Chem. Phys.*, 2013, 15, 3752-3763.

87. H. Paulsen, V. Schuenemann and J. A. Wolny, *Eur. J. Inorg. Chem.*, 2013, 628-641.

88. K. Boukheddaden, *Eur. J. Inorg. Chem.*, 2013, 865–874.

89. D. Chiruta, J. Linares, Y. Garcia, P. R. Dahoo and M. Dimian, *Eur. J. Inorg. Chem.*, 2013, 3601–3608.

90. D. Chiruta, J. Linares, M. Dimian and Y. Garcia, *Eur. J. Inorg. Chem.*, 2013, 951–957.

91. A. Rudavskyi, C. Sousa, C. de Graaf, R. W. A. Havenith and R. Broer, *J. Chem. Phys.*, 2014, 140, 184318.

This journal is © The Royal Society of Chemistry [year]

Chem. Soc. Rev., [year], **[vol]**, 00–00 | **12**

* Colour graphic: maximum size 8 cm x 4 cm:

Spin crossover with thermal hysteresis

5 * Text: one sentence, of maximum 20 words, highlighting the novelty of the work:

Memory applications of spin crossover require bistability: magnetic data must be appropriately collected and reported, and consideration given to lifetimes.

10

* Biography:

Professor Sally Brooker (FRSNZ, FNZIC, FRSC) went to Hawarden Area School (1970-1982), then studied at the
15 University of Canterbury, New Zealand [BSc(Hons) first class; PhD with Professor Vickie McKee]. After postdoctoral research at Georg-August-Universität Göttingen, Germany with Professor George M. Sheldrick, she took up a Lectureship at the University of Otago where she is now a Professor. Her research interests
20 concern the design, synthesis and full characterisation of, primarily paramagnetic, di- and poly-metallic complexes of transition metal ions with polydentate acyclic and macrocyclic ligands, as these have interesting redox, magnetic, catalytic and photophysical   properties
25 (http://neon.otago.ac.nz/research/sab/sab-res.htm).

30